COMPUTATION OF PHOTOSYNTHETICALLY USABLE RADIATION IN TURBID WATERS

Boredin SAENGTUKSIN*[a], Chew Wai CHANG[b], Soo Chin LIEW[c]

[a]*Associate Scientist, Centre for Remote Imaging, Sensing and Processing (CRISP), National University of Singapore, 10 Lower Kent Ridge Road, Blk S17 Level 2, Singapore 119076*
Tel: (65) 6515 4145; Email: boredin@nus.edu.sg

[b]*Research Scientist, CRISP*
Tel: (65) 6516 4322; Email: solomonchang@nus.edu.sg

[c]*Principal Research Scientist and Head of Research, CRISP*
Tel: (65) 6515 5069; Email: scliew@nus.edu.sg

KEY WORDS: downwelling irradiance, inherent optical properties, photosynthetically usable radiation

ABSTRACT: This paper describes how the depth-dependent photosynthetically available radiation (PUR) can be derived for waters with various types of suspended particles and turbidity values. Using a Mie-scattering routine, we compute the wavelength-dependent scattering phase functions and scattering cross-sections for a suspension of particles in water following the Junge-type particle size distributions. The particles are assumed to compose of various proportions of silt, clay and sand particles. The inherent optical properties are then calculated. These optical properties are used to simulate the downwelling spectral irradiance and photon flux density at various depths, by using the "Hydrolight" radiative transfer software package. PUR is calculated by weighting the downwelling photon flux density with a normalized chlorophyll absorption spectrum from the PROSPECT package and then integrated over the visible wavelength region. Our results indicate that the PUR generally decreases exponentially with depth for all suspension types and turbidities considered. In addition, we demonstrate that in clear waters, it typically takes more than 10m for the PUR to decrease to one-tenth of its just-below-surface values. In more turbid waters, however, it takes less than 2m for the PUR to show the same decrease.

INTRODUCTION

The photosynthetically available radiation (PAR) is useful for modeling the primary production of green vegetation including the underwater vegetation such as seagrass and algae. The PAR is defined as the broadband downward photon flux density integrated over the visible wavelength region from 400 nm to 700 nm (usually expressed in units of micromole of photons per square meter). As light propagates through water, the spectral content of the photon flux changes with depth due to the wavelength dependence extinction coefficient. As the depth increases, the photon flux tends to peak in the green region. However, since chlorophyll absorbs primarily in the blue and red regions of the visible spectrum, the photosynthetically usable radiation (PUR) would vary with depth and water quality parameters.

Suspended particulate matter plays a critical role in the propagation of underwater light field [Boss et al, 2009]. These suspended particles influence the light fields mainly through their scattering properties, which are characterized by their spectral scattering coefficient, $b(\lambda)$, and spectral scattering phase function, $P(\lambda, \theta)$, where λ is the wavelength in air and θ is the scattering angle. These inherent optical properties (IOPs) are dependent on the types of particles and their concentrations in the water. Therefore, the PUR is affected by the particle suspension. In this paper, we describe how the depth-dependent PUR in waters of various particle suspensions and turbidities are derived, and provide brief discussions on how the PUR is influenced by these factors.

First, various Junge-type particle size distributions (PSDs) are generated from lognormal populations of clay, silt and sand particles, which are mineral particles ubiquitous in natural waters. 3 lognormal PSDs are summed into one Junge-type PSD—this gives physical meaning to the mixing of three particle groups into one suspension and negates the need for unrealistic and arbitrary partitioning of the Junge-type PSD into separate particle types. Wavelength-dependent refractive indices are then used to generate the scattering IOPs of each particle type; the spectral absorption coefficient, $a(\lambda)$, are generated from a spectral model for gelbstoff [IOCCG, 2000]. These IOPs are then used to simulate the downwelling irradiance, $E_d(\lambda)$, by using the radiative transfer software package Hydrolight [Mobley and Sundman,

2006]. Finally, the PUR is computed by weighting $E_d(\lambda)$ with a normalized chlorophyll absorption spectrum from the PROSPECT model [Jacquemond et al, 1990].

METHODS AND PROCEDURES

A Junge-type PSD is described by the power law equation

$$n(r) = n_0 \left(\frac{r}{r_0}\right)^{-\gamma} \quad , \qquad (1)$$

where r is the radius of the particle, which is assumed spherical, n_0 is the number concentration at the reference radius r_0 (taken to be 1μm), and γ is the slope factor of the PSD, typically reported to be in the range 3 to 5 [Jonazs and Fournier, 2007]. The unit of $n(r)$ is usually given as the number of particles per unit volume per radius interval. Populations of clay, silt and sand particles are described by the lognormal distribution

$$n_i(r) = \frac{N_i}{r s_i \sqrt{2\pi}} e^{-\frac{(\ln r - m_i)^2}{2 s_i^2}} \quad , \qquad (2)$$

where m_i and s_i are respectively the mean and standard deviation of $\ln r$ of the i-th component, while N_i is the total number of particles of type i per unit volume of the suspension. An optimization routine was used to generate Junge-type PSDs from the summation of 3 lognormal PSDs. In the optimization, each particle is constrained to have its mean radius within the size interval which defines that particle type: clay particles in the ≤1μm range, silt particles in the 1μm-25μm range, and sand particles in the ≥25μm range [Parker, 2009]. 5 Junge-type PSDs were generated, for γ = 3.0, 3.5, 4.0, 4.5, and 5.0. All 5 resulting PSDs fit very well with Junge power law, with R^2 values all >0.99.

The single particle scattering properties are computed using a Mie scattering routine (BHMIE) [Bohren and Huffman, 1983]. The scattering coefficient $b(\lambda)$ is

$$b(\lambda) = \int_{r_{min}}^{r_{max}} Q_s(r,\lambda) \pi r^2 n(r) dr \quad , \qquad (3)$$

where $Q_s(r,\lambda)$ is the single particle scattering efficiency calculated by BHMIE, and r_{min} and r_{max} are respectively the minimum and maximum radius of particles in the suspension. The volume scattering function is

$$\beta(\lambda,\theta) = \frac{1}{k^2} \int_{r_{min}}^{r_{max}} S_{11}(\lambda,\theta,r) n(r) dr \quad , \qquad (4)$$

where the amplitude scattering matrix element $S_{11}(\lambda,\theta,r)$ is also calculated by BHMIE, $k = 2\pi/\lambda$ is the wavenumber in water. The phase function is then the ratio $P(\lambda,\theta) = \beta(\lambda,\theta)/b(\lambda)$. Note that the integral of the phase function over all direction is normalized to 1. The above series of steps allows us to generate the scattering IOPs of the suspension. The absorption coefficient is obtained from a spectral model of gelbstoff.

In this work, we have used the backscattering coefficient at 550nm, $b_b(550)$, as a proxy to the water's turbidity [Hu et al, 2003]. Further, in order to isolate the effects of the suspension type on the downwelling irradiance at each turbidity level, $b_b(550)$ is fixed to be the same across the 5 PSDs. Four turbidity levels are simulated, according to the $b_b(550)$ values shown in Table 1. These IOPs are input into Hydrolight to calculate the downwelling irradiance at various depths ranging from 0 m (immediately subsurface) to 12.8 m. The waters are assumed to be vertically homogeneous. The downwelling irradiance computed are finally weighted with the normalized chlorophyll absorption spectrum from the PROSPECT leave model to produce the PUR, which is integrated over the visible range (400-750nm) and computed in quantum units, ie. μmol of photons per second per square meter.

Turbidity level	$b_b(550)$ / m^{-1}
Low	0.05
Moderate	0.2
High	0.5
Very high	1.0

Table 1: the four turbidity levels simulated and their corresponding $b_b(550)$ values

RESULTS AND DISCUSSION

The following graph shows the backscattering coefficient, normalized to one at 550nm, for the 5 PSDs.

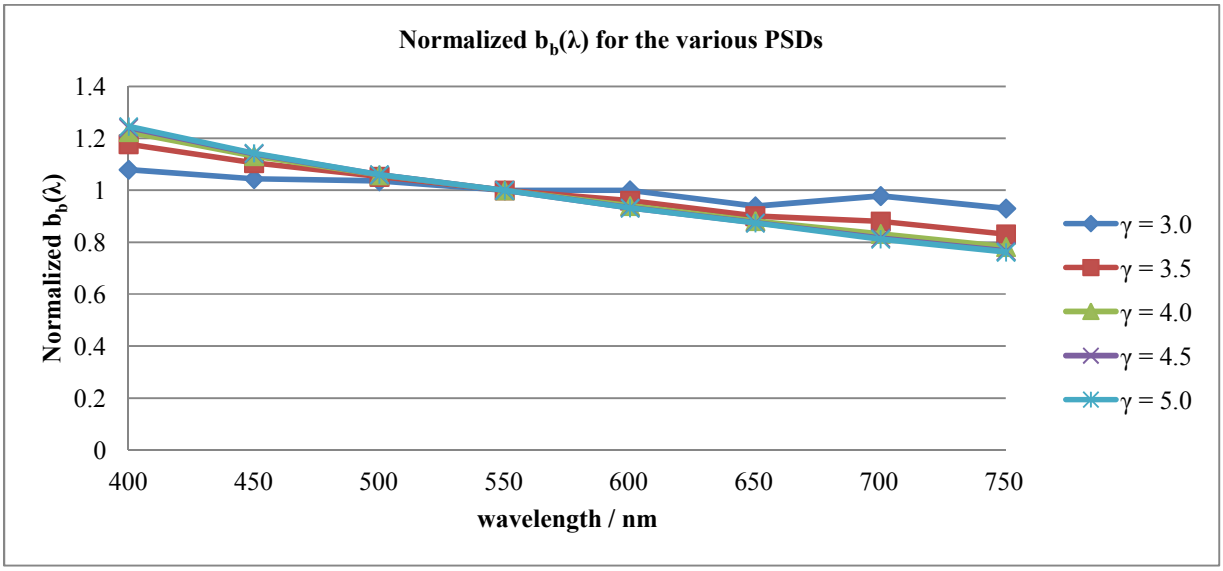

Fig 1: backscattering coefficient of the various PSDs, normalized at 550nm.

From the graph above, we can easily obtain $b_b(\lambda)$ for the various turbidity levels by multiplying the value of $b_b(550)$. It is noted from the graph that the $b_b(\lambda)$ profiles display limited differences across the PSDs, and that the spectral dependence of $b_b(\lambda)$ increases with γ. This suggests that suspensions with higher proportions of small particles are more sensitive to wavelength changes. Fig 2 below shows the PUR as a function of depth for all PSDs, at moderate turbidity.

All simulated PUR fall in the range that is typically measured in natural water bodies [Kirk, 1986]. The key results of our simulations are that, firstly, the PUR decreases exponentially with depth for all turbidity levels (only the moderate turbidity level is shown in Fig 2) and suspension types considered, with all PUR profiles showing very good fits ($R^2 >$ 0.99) to the exponential relation. Secondly, the PUR at all depth is predominately determined by the backscattering coefficient (and hence the turbidity level), and the suspension type has very minimal influence. This may be expected: downwelling irradiance is attenuated by $a(\lambda)$ and $b_b(\lambda)$, but is less dependent on the detailed profile of the phase function and $b(\lambda)$. Therefore, although the $b(\lambda)$ spectra and phase functions are different between the 5 PSDs, their backscattering coefficient spectra show limited differences (see Fig 1), resulting in minimal differences in $E_d(\lambda)$ and hence PUR.

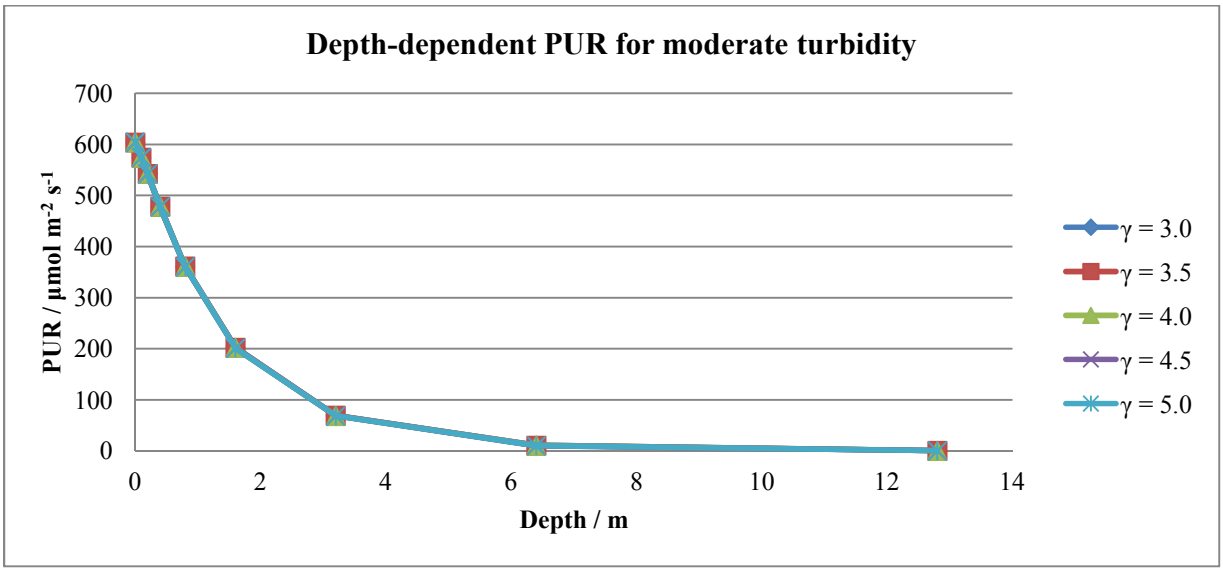

Fig 2: depth-dependent PUR in moderately turbid water, for all PSDs.

An important aspect of the downwelling irradiance is its direct influence on the euphotic zone, which is usually defined as the depth to which the downwelling irradiance is attenuated to 1% of its subsurface value, while the mid-point of the euphotic zone is the depth to which the downwelling irradiance is attenuated to 10% [Kirk, 1986]. Here, we have calculated the euphotic zone and its mid-point based on the PUR. The table below shows the mid-point depth for the waters with various Junge-type PSDs and turbidity.

Turbidity	γ = 3.0	γ = 3.5	γ = 4.0	γ = 4.5	γ = 5.0
Low	10.41	10.40	10.36	10.34	10.34
Moderate	3.95	3.95	3.94	3.93	3.93
High	2.09	2.09	2.08	2.08	2.08
Very high	1.28	1.28	1.28	1.28	1.27

Table 2: the depth (m) where PUR is attenuated to 10% of the subsurface value.

It can be seen that in waters of low turbidity, it takes more than 10m for the PUR to attenuate to 10% of its subsurface value, but this depth quickly decreases as turbidity increases, to as low as 1.3m in waters of very high turbidity. Taken together, our results show that the depth to which aquatic photosynthesis can take place is highly dependent on the turbidity of the water body; on the other hand, the effects of differing compositions of clay, silt and sand particles are small, if the overall PSD is of the Junge-type.

CONCLUSION

We have described in this paper how the depth-dependent PUR can be computed in waters of various particle suspension types and turbidity levels. Three types of mineral particles have been considered (clay, silt and sand particles), with each overall suspension being characterized as Junge-type PSD. Scattering IOPs of each suspension have been calculated from Mie scattering, while the absorption coefficients are taken from a spectral model. These wavelength-dependent IOPs are then used to simulate for the downwelling irradiance at various depths using Hydrolight, after which the downwelling irradiance is converted to the PUR using a chlorophyll absorption model.

Our simulation results indicate that PUR decreases exponentially with depth for all turbidity levels and PSDs tested. In addition, the turbidity level is a very strong factor that influences the depth of irradiance penetration: in clear waters, it typically takes more than 10 m for the PUR to decrease to one-tenth of its just-below-surface values, whereas this depth decreases to less than 2m in waters of high turbidity. This strong influence on aquatic photosynthesis translates to strong effects on other ecosystem-level biophysical phenomena, as well as other processes such as heat and nutrients cycling.

The type of suspension, however, has limited impacts on the PUR. As explained in the text, this is likely because PUR is a "broad" quantity that is not strongly dependent on the exact profile of the phase functions. In the 5 Junge-type PSDs simulated, the differences in the phase functions do not manifest strongly in the backscattering coefficient spectra, leading to $b_b(\lambda)$ values that are not significantly different. Efforts are on-going to consider other particle types, such as phytoplankton, as well as other PSDs, including those that deviate from the Junge-type power law.

REFERENCES

Boss E., Taylor L., Gilbert S., Gunderson K., Hawley N., Janzen C., Johengen T., Purcell H., Robertson C., Schar D. W. H., Smith G. J., and Tamburri M. N., 2009. Comparison of inherent optical properties as a surrogate for particulate matter concentration in coastal waters, Limnol. Oceanogr. Methods, Vol 7, pp803-810.

Hu, C., Lee, Z., Muller-Karger, F.E., Carder, K.L., 2003. Application of an optimization algorithm to satellite ocean color imagery: a case study in southwest Florida coastal waters. Proc. Ocean Remote Sensing and Applications. SPIE – The International Society for Optical Engineering 4892, 70-79.

IOCCG, 2000. Remote Sensing of Ocean Colour in Coastal, and Other Optically-Complex Waters. Sathyendranath, S. (ed.), Reports of the International Ocean-Colour Coordinating Group, No. 3, IOCCG, Dartmouth, Canada.
Kirk J. T. O., (1986). Light and Photosynthesis in Aquatic Ecosystems, Cambridge Univ. Press, New York.

Jacquemoud S. and Baret F., 1990. PROSPECT: A model of leave optical properties spectra, Remote Sens. Of Environ., 34: pp75-91.

Jonasz M. and Fournier G. R., 2007. Light Scattering by Particles in Water: Theoretical and Experimental Foundations, Academic Press, New York.

Mobley C. D. and Sundman L. K., 2006. Hydrolight 4.3 Users' Guide, Sequoia Scientific Inc, Bellevue, WA.

Parker R. 2009. Plant and Soil Science: Fundamentals and Applications, Delmar Cengage Learning, New York.
Bohren C. F. and Huffman D. R., (1983). Absorption and scattering of light by small particles, J. Wiley & Sons, New York.